Electronic structures of Mg_3Pn_2 (Pn=N, P, As, Sb and Bi) and Ca_3N_2 calculated by a first-principle pseudopotential method

Y. IMAI*, A. WATANABE
National Institute of Advanced Industrial Science and Technology, AIST Tsukuba Central 5, Higashi 1-1, Tsukuba, Ibaraki 305-8565, Japan
E-mail: imai-y@aist.go.jp

Published online: 3 March 2006

Electronic structure calculations for Mg_3N_2, Mg_3P_2, Mg_3As_2 (low and high temperature modifications), Mg_3Sb_2, Mg_3Bi_2, and Ca_3N_2 have been performed. Mg_3Sb_2 is predicted to be an indirect semiconductor with the gap value of about 0.41 eV. Mg_3As_2 with a high temperature modification is also predicted to be a semiconductor with the gap value of about 1.1 eV, but the valence band maximum and the conduction band minimum of Mg_3Bi_2 contacts at Γ which would make it a semimetal. Mg_3N_2, Mg_3P_2, and Mg_3As_2 (low temperature phase) are semiconductors with the direct band gaps of 1.64 eV, 1.73 eV, and 1.57 eV, respectively. Ca_3N_2 is a semiconductor with a gap of about 1.2 eV. © *2006 Springer Science + Business Media, Inc.*

1. Introduction

Alkaline earth (AE) metals (Mg, Ca, Sr and Ba) are known to form semiconducting compounds with Si, such as Mg_2Si, Ca_2Si, and $BaSi_2$. They are recently attracting attention as ecologically friendly semiconductors [1–3].

Among them, Mg_2Si has already been investigated as a thermoelectric (TE) material [4, 5] but its TE figure of merit is inferior to Bi-Te alloys conventionally used because its heat conductivity is high. Compounds composed of light elements, such as Mg and Si, tend to have large lattice heat conductivities and this is unfavorable for high TE performance. Solid solutions of Mg_2Si-Mg_2Ge have been investigated so as to avoid this disadvantage, and they have been known to have a remarkably low heat conductivity compared to Mg_2Si or Mg_2Ge [6]. A substituted solid solution is considered to have a strong point defect scattering of phonon due to the large mass difference, and the synthesis of $Mg_2Si_{1-x}Ge_x$ has been the target of recent investigations [7, 8].

Recently, Kajikawa *et al*. proposed that semiconducting Mg pnictides can be TE material candidates [9] because they are composed of elements heavier than Si or Ge and would have lower lattice thermal conductivities. They confirmed that the thermal conductivity of the Mg_3Sb_2 sintered at 1253 K is less than 2 W/mK at 500–600 K, which is lower than that of $Mg_2Si_{0.6}Ge_{0.4}$, the compositions with the lowest thermal conductivity among the $Mg_2Si_{1-x}Ge_x$ alloys [6]. Therefore, Mg_3Sb_2 was considered to be promising for TE materials in the temperature range from 400 to 700 K.

Mg is known to form a series of intermetallic compounds with the 15th Group elements (Pnicogens (Pn); N, P, As, Sb and Bi), the formulas of which are expressed as Mg_3Pn_2. If their semiconducting gaps are favorable, the TE performances of their solid solutions would be better since their heat conductivities will be further reduced.

However, their electronic structures have not yet been fully clarified. Previous electronic structure calculations for Mg_3Pn_2 have been limited to Mg_3N_2, Mg_3Bi_2 and Mg_3Sb_2.

As for Mg_3N_2, Fang *et al*. concluded that this has a direct energy gap of 1.1 eV using the localized spherical wave method [10]. However, Mg_3N_2 has an open structure, and it is generally admitted that compounds with open structures are hard to be treated by the atomic sphere approximation because the one-electron potential lacks in spherical symmetry outside the overlapping sphere centered about each atom. Armenta *et al*. stated that this has a direct gap of 2.26 eV using the self-consistent field periodic Hartree-Fock (HF) LCAO procedures [11]. They also stated that the indirect gap between Γ (the valence band maximum) and the conduction band minimum at the point along the Γ-*N* is 2.25 eV, but it should be noted that the

*Author to whom all correspondence should be addressed.

0022-2461 © *2006 Springer Science + Business Media, Inc.*
DOI: 10.1007/s10853-006-5181-3

TABLE 1 Crystallographic data of the compounds calculated in the present study

	Nominal composition in a unit cell	Space group number	Lattice constant, a (nm)	Lattice constant, c (nm)
Mg_3N_2	$Mg_{48}N_{32}$	206	0.9964	–
Mg_3P_2	$Mg_{48}P_{32}$	206	1.201	–
Mg_3As_2 (low)	$Mg_{48}As_{32}$	206	1.233	–
Mg_3As_2 (high)	Mg_3As_2	164	0.4264	0.6738
Mg_3Sb_2	Mg_3Sb_2	164	0.4573	0.7229
Mg_3Bi_2	Mg_3Bi_2	164	0.4666	0.7401
Ca_3N_2	$Ca_{48}N_{32}$	206	1.1473	–

HF method has a tendency to overestimate the band gap due to the neglect of screening for coulomb interactions. Orhan *et al*. stated that the gap is 1.63 eV using the full potential linearized augmented plane wave (FP-LAPW) method [12]. The variation in these predicted gap values is quite high.

As for Mg_3Bi_2 and Mg_3Sb_2, Watson *et al*. [13] calculated the electronic structure for the first time using the Extended 'Hückel' method and discussed the results of the X-ray emission spectra but did not give a gap value since the 'Hückel' method may give quantitatively inaccurate results. Though Xu *et al*. [14] concluded that Mg_3Sb_2 is a semiconductor with the gap of 0.12 eV using the augmented spherical wave (ASW) method, it also has an open structure, and spherical wave method may not be appropriate for this compound, as in the case of Mg_3N_2.

There are no reports on the calculations of the electronic structures of Mg_3P_2 and Mg_3As_2 to our knowledge, though the observed gap value of Mg_3As_2 is 2.2 eV [15].

In the present paper, the results of systematic calculations of Mg_3Pn_2 using the plane wave method will be given. Preparatory discussions about the Ca-Pn systems will also be presented.

2. Compounds considered

Mg_3Pn_2 are known to have either the crystal structure of; a cubic structure of the Mn_2O_3 type or a hexagonal structure of the La_2O_3 type [16, 17]. The unit cell of the former is composed of 80 atoms, 48 Mg and 32 Pn, and belongs to the space group of I_{a3} (206), which can be reduced to the primitive cell composed of 40 atoms. The unit cell of the latter is composed of 5 atoms, 3 Mg and 2 Pn, and belongs to the space group of P_{3m1} (164). Mg_3N_2 and Mg_3P_2 are known to have the Mn_2O_3-type structure. Mg_3As_2 also has this type of structure at ambient temperature, but changes to the La_2O_3-type structure at about 1323 K. On the contrary, Mg_3Sb_2 has the La_2O_3-type structure below 1203 K, but has the Mn_2O_3-type structure above that temperature. Mg_3Bi_2 has also La_2O_3-type structure at the ambient temperature.

As for the Ca-Pn systems, Ca_3N_2 has the cubic Mn_2O_3-type structure, but there are still discussions about the stoichiometric compositions of Ca_3P_2, Ca_3As_2, Ca_3Sb_2 and Ca_3Bi_2. As for the Ba-Pn compounds, some authors state the existence of Ba_3P_2, Ba_3As_2, and Ba_3Sb_2, but their structures have not yet been determined. Therefore, the following compounds are considered as targets of

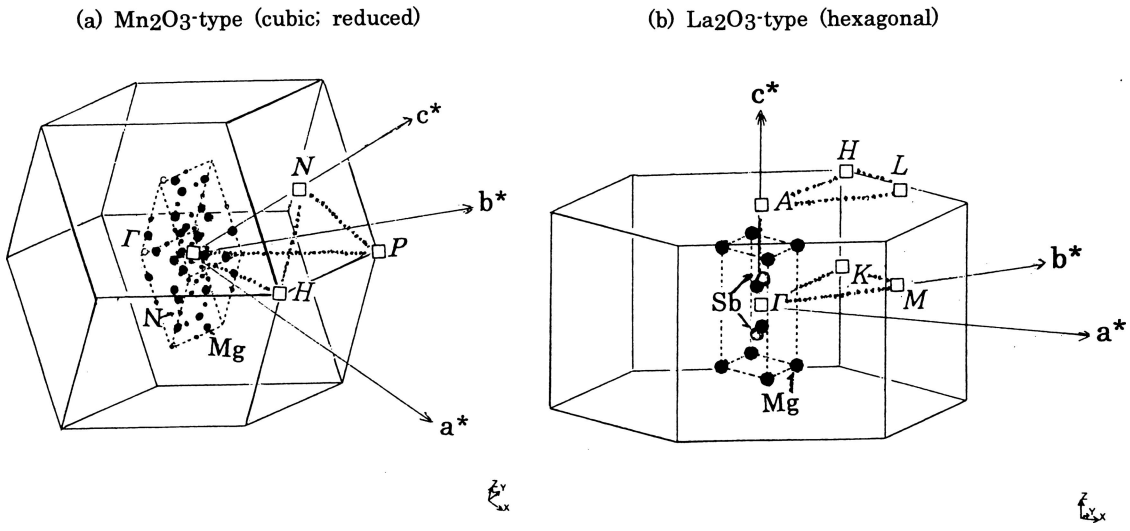

Figure 1 *Crystal* structure and the Brillouin zone of (a), the Mn_2O_3-type structure, and (b), the La_2O_3-type structure. Dashed lines indicate the unit cell of Mg_3N_2 in Fig. (a), where Mg and N are denoted by larger and smaller circles, respectively. In Fig. (b), dashed lines indicate the unit cell of Mg_3Sb_2, where Mg and Sb are denoted by closed and open circles, respectively. Solid lines indicate the Brillouin zone boundaries. Chosen sets of reciprocal space points with high symmetry are shown by open squares. Dotted lines indicate the paths along which the calculations of the band structure have been performed.

the present calculations; Mg_3N_2 (Mn_2O_3-type), Mg_3P_2 (Mn_2O_3-type), Mg_3As_2 (Mn_2O_3-type and La_2O_3-type), Mg_3Sb_2 (La_2O_3-type), Mg_3Bi_2 (La_2O_3-type), and Ca_3N_2 (Mn_2O_3-type)

Crystallographic data (space group number and lattice constants) of the compounds treated in the present study are collected from handbooks [15, 16] and summarized in Table 1. Fig. 1 is schematic drawings of the unit cell and the Brillouin zone of (a), the Mn_2O_3 type structure, and (b), the La_2O_3-type structure, in which the cubic unit cell is reduced to the rhombohedral primitive cell in (a).

3. Calculation methods

The calculation methods are the same as those used in the previous studies [18–20]. That is, the code of CASTEP (CAmbride Serial Total Energy Package) [21] has been used, which is a first-principle pseudopotential method based on the density-functional theory (DFT) for describing the electron-electron interaction, a pseudopotential description of the electron-core interaction, and a plane-wave expansion of the wavefunctions. The pseudopotential used is the ultrasoft pseudopotential generated by the scheme of Vanderbilt [22] which is bundled in the Cerius2[1] graphical User Interface.

As for the method of approximation to the exchange-correlation term of the DFT, the local density approximation (LDA) with the generalized gradient correction [23] was used. The kinetic cutoff energy for the plane wave expansion of the wavefunctions was set at 250 eV, which was confirmed to be sufficient to obtain well-converged DOS curves with respect to the cutoff energy.

The DOS curves were obtained by broadening the discrete energy levels using a Gaussian smearing function of 0.07 eV full-width at half-maximum (FWHM) on a grid of *k*-points generated by the Monkhorst-Packe scheme [24] with a *k*-point spacing of 0.5 nm^{-1} or less. The energies are shifted so that the Fermi energies (E_Fs) are aligned with zero in the DOS figures.

All of the angular momentum projections (‘*s*, *p*, *d*’.) on all the atoms are also performed to give a partial density of states (PDOS). The units of DOS are electrons/(cell eV) for the total DOSs and electrons/(atom eV) for the PDOSs. The site dependence of the PDOS of the same kind of atoms could be roughly ignored.

Calculations of the band structure (BS) along several high-symmetry lines in the Brillouin zone have also been conducted.

4. Results and discussion

4.1. Mg_3Pn_2 with the La_2O_3-type structure

At first, we present the calculated results for Mg_3Sb_2 in Fig. 2, which is a TE material candidate. The energies are measured with respect to the Fermi level. The Mg2*p*

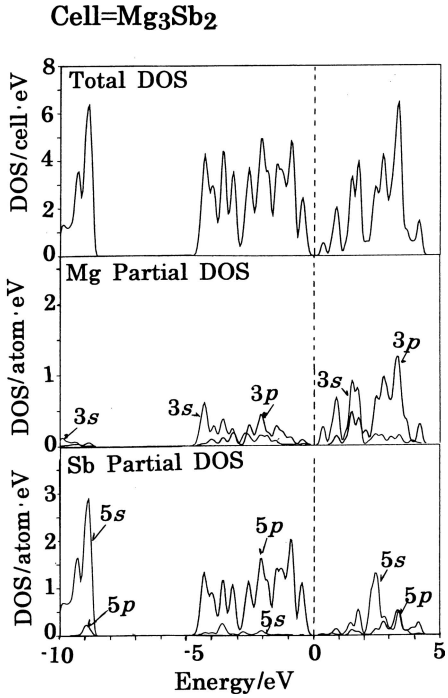

Figure 2 Total and Partial DOSs of Mg_3Sb_2. Dashed lines (0 eV) in this and succeeding figures indicate the Fermi levels of the compounds unless otherwise specified.

states located around –45 eV are omitted though they are included in the calculation as valence states. As shown in the top of Fig. 2, the valence bands extend down to about 10 eV below the Fermi level (E_F; 0 eV, shown by a broken line), and can be divided into two main parts; a part located at about –9 eV or below and a part located at about from –5 eV to 0 eV. Above the gap of about 0.4 eV, one can find the conduction band.

The details of the PDOSs near E_F are shown in the middle and the bottom of Fig. 2. As is clearly seen, the lower valence bands are mainly composed of Sb5*s*. The uppermost valence bands are mainly composed of Sb5*p*, hybridized with Mg3*s* and Mg3*p*. The conduction bands are of Sb5*s*, Mg3*s*, and Mg3*p*.

Fig. 3 shows the band structure (BS) of Mg_3Sb_2 along the high symmetry directions of the Brillouin zone near the Fermi level. Plotted in the BS figure are the numbers which express the order counted from the bottom of the valence band. The band gap is indirect with the top of the valence band (the 17th band) at Γ and the bottom of the conduction band (the 18th band) at *K*. The gap value is about 0.41 eV.

The present results are qualitatively the same as the previous study by Xu *et al.* [14], but there are some differences in the details. According to them, the bottom of the conduction band is located along the line *M*-*L* and the calculated indirect gap was 0.12 eV, as stated above. Our calculation also suggested that there is an energy minimum for the lowest conduc-

[1]Cerius[2] is a trademark of Accelrys, Inc.

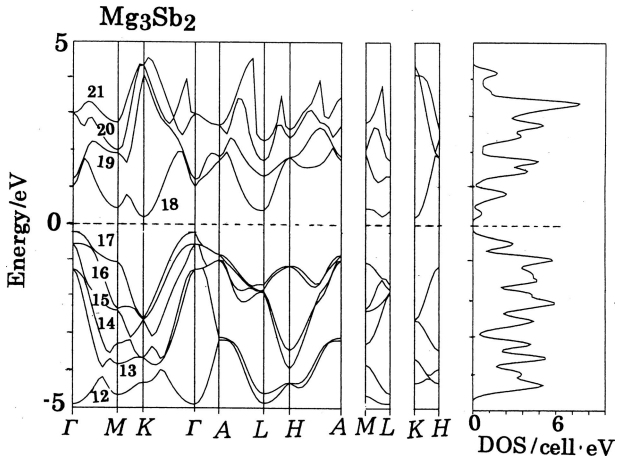

Figure 3 Band structure of Mg_3Sb_2. Plotted in the BS figure are the numbers which express the order counted from the bottom of the valence band. It should be noted that the Mg2*p* states are explicitly treated as a part of the valence. The 1st to the 9th bands located at about –45 eV composed of Mg2*p* orbitals and the 10th to 11th bands composed of Sb5*s* orbitals are omitted in this figure and the numbering starts from 12.

tion band, the 18th band, along the line *M*-*L* and the energy there is very close to that at *K*, but 0.04 eV higher, and the bottom of the conduction band is located at *K*.

There seems to be no recent measurements of the band gap of crystalline Mg_3Sb_2. However, Verbrugge and Zytveld [25] estimated the gap of the liquid phase of Mg_3Sb_2 as 0.8 eV. A half century ago, Busch *et al.* reported the value of 0.82 eV for the solid Mg_3Sb_2 [26].

Both of our prediction and Xu *et al.*'s [14] cited above are lower than this value. However, our value seems to be reasonable if we allow the tendency that about 50% of the measured gap is often obtained in the LDA calculations. Xu *et al.*'s gap value of 0.12 eV seems to be too low.

Fig. 4 shows the band structure of Mg_3As_2 in the high temperature modification, (a), and Mg_3Bi_2, (b), both of which have the La_2O_3type structure, near their Fermi levels.

Here, the valence band maximum is chosen as the zero of the energy so as to clarify the difference between them.

Fig. 4a, the band structure of Mg_3As_2 in the high-temperature modification, shows that the top of the valence band is located at Γ. The energy minimum of the lowest conduction band, the 18th band, is also located at Γ. The energy gap between Γ_{17} and Γ_{18} is estimated to be 1.1 eV. However, the energy difference between the Γ, *K* and the state along the line *M*-*L* of the 18th band is about 0.05 eV or less and it is difficult to state definitely that the gap is direct or indirect.

In Fig. 4b, the band diagram of Mg_3Bi_2, we find contact of the valence band maximum and the conduction band minimum at Γ. Therefore, it is predicted to be a semimetal. This result is the same as that of the non-relativistic calculation by Xu *et al.*'s [14].

Therefore, the turn of the band gaps of these are as follows: $Mg_3As_2 > Mg_3Sb_2 > Mg_3Bi_2$.

4.2. Mg_3Pn_2 with the Mn_2O_3-type structure

As stated above, Mg_3As_2 (low temperature phase), Mg_3P_2, and Mg_3N_2 have the Mn_2O_3 type structure. Fig. 5 shows their calculated band structure. The numbers beside the BS figure express the order counted from the bottom of the valence band. The 1st to the 72nd bands located at about –42 eV are composed of the Mg2*p* orbitals and the 73rd to 88th bands composed of the As4*s*, P3*s* or N2*s* orbitals are omitted in these figures and the numbering starts from 89.

As are shown, they are all semiconductors with the direct band gaps of 1.64 eV (Mg_3N_2), 1.73 eV (Mg_3P_2), and 1.57 eV (Mg_3As_2).

Fang *et al.* [10] and Reckeweg *et al.* [27] determined the energy gap of Mg_3N_2 to be 2.8 eV using optical diffuse-reflectance spectra. Our result for Mg_3N_2 is close to Orhan et al'.'s previous value of 1.63 eV [12] but is about 60% of the observed value, as is often the case when using

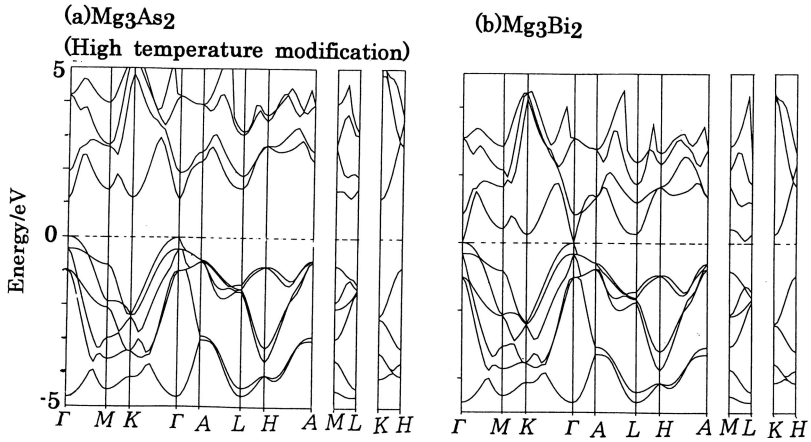

Figure 4 Band structures of Mg_3As_2 in the high temperature modification, (a), and of Mg_3Bi_2. The valence band maximum is chosen as the zero of the energy.

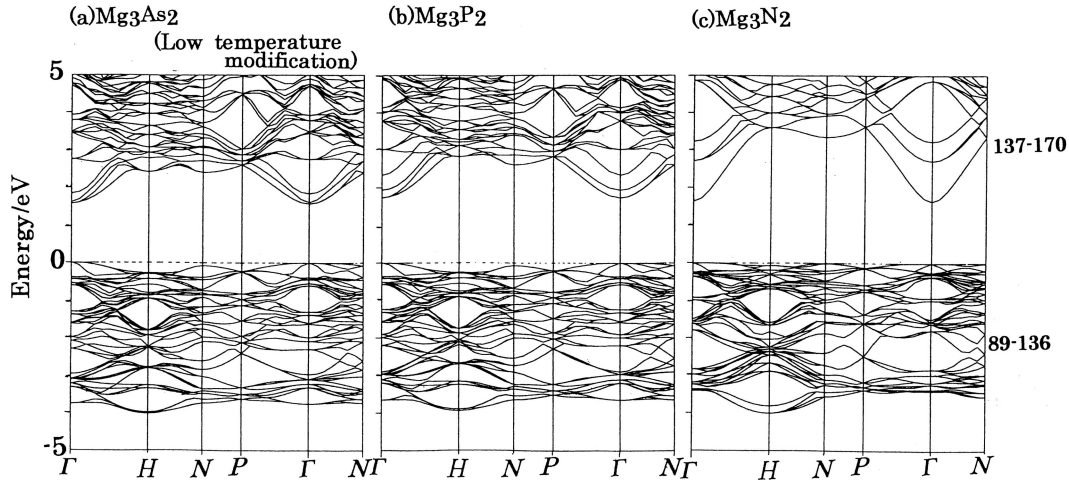

Figure 5 Band structures of Mg_3As_2 in the low temperature modification, (a), Mg_3P_2, (b), and, Mg_3N_2 (c). The valence band maximum is chosen as the zero of the energy.

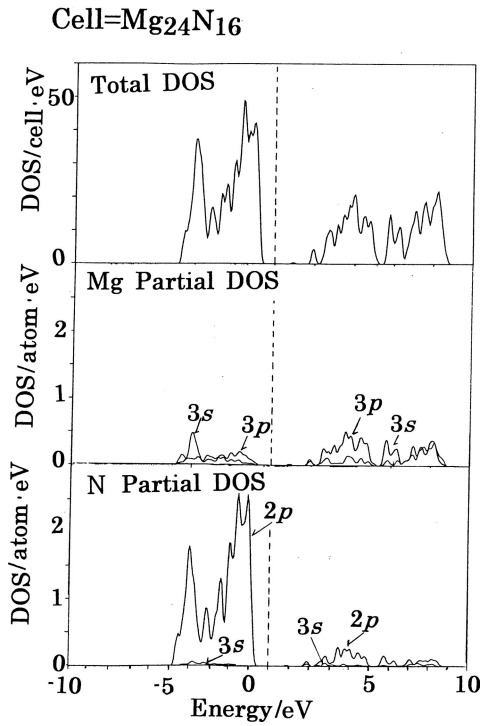

Figure 6 Total and partial DOSs of Mg_3N_2.

the density functional method. Armenta *et al.*'s value of 2.25 eV using the HF method [11], which has a tendency to overestimate the value, was closer to the observed value in the present case.

As for Mg_3As_2, our value calculated is about 70% of the observed value of 2.2 eV [15]. There are no available data for the observed gap value of Mg_3P_2 as a comparison.

One may assume that a monotonic shift for a band gap in the systematic calculations going from Mg_3N_2 to Mg_3P_2 and to Mg_3As_2 would be natural as in the case of Mg_3Pn_2 with the La_2O_3-type structure. The reason for the difference in the expected tendency and the calculated result is not clear at present, but there are several factors which may influence the gap value. For example, Larson *et al.* [28] carried out systematic calculations of the electronic structure of YNiPn where Pn is a pnicogen element. A decrease in the gap was observed as one goes from As to Bi. On the contrary, broadening of the band gap upon going to heavier elements is observed in the series of transition metal disilicides and sesqui-silicides, which may be caused by the enhanced effect of hybridization in the heavier elements for which the energy difference between higher orbitals is smaller [29]. The apparent complex tendency of the gap broadening in the present case may be caused by these opposite factors. A similar case is observed in the calculated band gaps of Mg_2Si, Mg_2Ge and Mg_2Sn [30]. In addition, relativistic effect (mass-velocity term and Darwin term) will predict complex effect on the band structures of the heavier element compounds [31] though the present calculations do not treat that explicitly but through the pseudopotentials.

Fig. 6 shows the total and the partial DOSs of Mg_3N_2. As is seen, the uppermost valence bands are mainly composed of N2*p*, with which Mg3*s* and Mg3*p* are hybridized. The bottom of the conduction bands are of N2*p* and Mg3*p*. The N3*s* bands in Mg_3N_2, which are composed of N3*s* bondingorbitals, are deeply located (−12 eV and below), though not shown here, which is comparable to the case of the Sb5*s* bands in Mg_3Sb_2 where the Sb5*s* bonding orbital is located at about –9 eV. The contribution of the N3*s* anti-bonding orbital to the conduction band is smaller if compared with that of the Sb5*s* anti-bonding orbitals.

4.3. Discussions about Ca-Pn systems

In Sections 4.1 and 4.2, the band gaps of Mg_3Pn_2 have been described. The gaps of Mg_3Pn_2, other than Mg_3Sb_2, seem to be too high for thermoelectric applications at mid-temperatures. Since the decrease in the gap value upon increasing the atomic weight is observed in some series

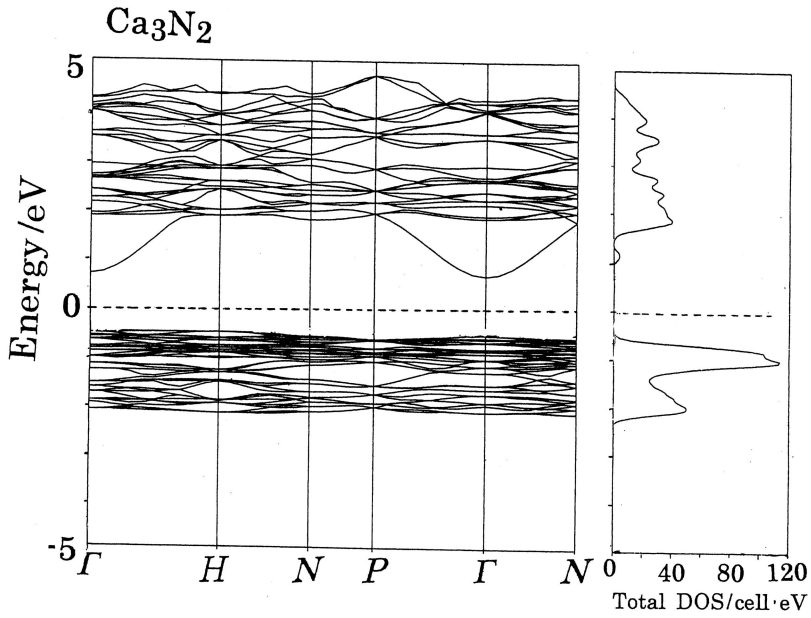

Figure 7 Band structure of Ca_3N_2.

of compound semiconductors as stated above, compounds with a suitable gap are expected by replacing Mg by Ca, Sr or Ba. However, the only compound with the composition of Ca_3Pn_2, which has been admitted to exist, is Ca_3N_2, as stated in Section 2.

The calculated band structure of Ca_3N_2 is shown in Fig. 7. The direct band gap is 1.20 eV at point Γ, which is slightly larger than the indirect gap ($\Gamma \rightarrow H$) of 1.18 eV. This result is almost the same as the recent work using the full potential-linearized augmented plane wave (FP-LAPW) method [32]. Since the gap of Ca_3N_2 is predicted to be narrower than that of Mg_3N_2 and both have the same crystal structure, the so-called "band-gap engineering technique" may be possible by replacing some Ca atoms with isoelectronic Mg. In addition, the disadvantage of the high thermal conductivity of Mg_3N_2 will be overcome by formation of the solid-solutions with Ca_3N_2. However, the band gap of Ca_3N_2 is still too high for thermoelectric application at mid-temperatures.

Ca_3As_2 and Ca_3Sb_2 would be, if present, favorable to form solid solutions with Mg_3Sb_2. Since the Ca-Pn compounds are more air-sensitive than the Mg-Pn compounds [33], the existence of Ca_3As_2, Ca_3Sb_2, (and Ca_3Bi_2) has not been displayed in the phase diagram [16]. However, Min and Sano claim that their formation was confirmed [34] as well as other previous investigators referred to in the phase diagram. Therefore, there still remains the possibility to form compounds with suitable band gaps of Ca (and Sr, Ba)$_3Pn_2$ and their solid solutions with each other or with Mg_3Pn_2.

5. Conclusion

The electronic structure calculations of Mg_3N_2 (Mn_2O_3 type), Mg_3P_2(Mn_2O_3type), Mg_3As_2 (low temperature phase, Mn_2O_3-type and high temperature phase, La_2O_3-type), Mg_3Sb_2(La_2O_3-type), Mg_3Bi_2(La_2O_3-type), and Ca_3N_2(Mn_2O_3-type) have been performed. Mg_3Sb_2 is predicted to be an indirect semiconductor with the gap value of about 0.41 eV. Mg_3As_2 in the high temperature modification is also predicted to be a semiconductor with the gap value of about 1.1 eV, but Mg_3Bi_2 is a semimetal. Mg_3N_2, Mg_3P_2, and Mg_3As_2 in the low temperature modification are semiconductors with the direct band gaps of 1.64 eV, 1.73 eV, and 1.57 eV, respectively. Ca_3N_2 is a semiconductor with the gap of about 1.2 eV.

Acknowledgments

The authors would like to express their sincere gratitude to Dr. Masaaki Sugie of National Institute of Advanced Industrial Science and Technology, Japan (AIST), for his kind technical assistance during the calculations. They are also grateful to TACC (Tsukuba Advanced Computing Center), AIST, for the financial support.

References

1. T. NAKAMURA, T. SUEMASU, K. TAKAURA, F. HASEGAWA, A. WAKAHARA and M. IMAI, *Appl. Phys. Lett.* **81** (2002) 1032.
2. H. MATSUI, M. KURAMOTO, T. ONO, Y. NOSE, H. TATSUOKA and H. KUWABARA, *J. Cryst. Growth* **237** (2002) 2121.
3. S. KISHINO, T. IIDA, T. KUJI and Y. TAKANASHI, *Thin Solid Films* **46** (2004) 90.
4. M. W. HELLER and G. C. DANIELSON, *J. Phys. Chem. Solid* **23** (1962) 601
5. T. KAJIKAWA, K. SHIDA, K. SHIRAISHI, M. OHMORI and T. HIRAI, *Mat. Sci. Forum.* **687** (1999) 308.

6. R. J. LABOTZ, D. R. MASON and D. F. O'KANE, *J. Electrochem. Soc*. **110** (1963) 127.
7. Y. NODA, N. OTSUKA, K. MASUMOTO and I. NISHIDA, *J. Jpn. Inst. Metals* **53** (1989) 487.
8. L. M. ZHANG, Y. G. LENG, H. Y. JIANG, L. D. CHEN and T. HIRAI, *Mat. Sci. Eng*. **B86** (2001) 195.
9. T. KAJIKAWA, N. KIMURA and T. YOKOYAMA, *Proc. 22*nd *Int. Conf. Thermoelectrics* (2003) 305.
10. C. M. FANG, R. A. DE GROOT, R. J. BRULS, H. T. HINTZEN and G. DE WITH, *J. Phys.- Condense. Mat*. **11** (1999) 4833.
11. M. G. M. ARMENTA, A. REYES-SERRATO and M. BORJA, *Phys. Rev*. **B62** (2000) 4890.
12. E. ORHAN, S. JOBIC, R. BREC, R. MARCHAND and J. -Y. SAILLARD, *J. Mater. Chem*. **12** (2002) 2475.
13. L. M. WATSON, C. A. W. MARSHALL and C. P. CARDOSO, *J. Phys. F: Met. Phys* **14** (1984) 113.
14. R. XU, R. A. DE GROOT and W. VAN DER LUGT, *J. Phys.-Condense. Mat*. **5** (1993) 7551
15. K. PIGON, *Helv. Phys. Acta* **41** (1968) 1104.
16. B. PREDEL, "Phase Equilibria, Crystallographic and Thermodynamic Data of Binary Alloys" in "Landolt-Boernstein Numerical Data and Functional Relationships in Science and Technology, New Series, Group IV, Volume 5, edited by O. Madelung (Springer-Verlag, Berlin) (1991–1998).
17. P. VILLARS and L. D. CALVERT, "Pearson's Handbook of Crystallographic Data for Intermetallic Phases" 2nd ed., Vol. 1–4, (ASM International, Ohio) (1991).
18. Y. IMAI, M. MUKAIDA, M. UEDA and A. WATANABE, *Intermetallics* **9** (2001) 721.
19. Y. IMAI, M. MUKAIDA, M. UEDA and A. WATANABE, *J. Alloys Compounds* **347** (2002) 244.
20. Y. IMAI and A. WATANABE, *Intermetallics* **11** (2003) 451.
21. M. C. PAYNE, M. P. TETER, D. C. ALLAN, T. A. ARIAS and J. D. JOANNOPOULOS, *Rev. Modern Phys*. **64** (1992).
22. D. VANDERBILT, *Phys. Rev*. **B41** (1990) 7892.
23. J. P. PERDEW and Y. WANG, *ibid*. **B33** (1986) 8800.
24. H. J. MONKHORST and J. D. PACK, *ibid*. **B13** (1976) 5188.
25. D. M. VERBRUGGE and J. B.VAN ZYTVELD, *J. Non-Crystalline Solids* **736** (1993) 156.
26. G. BUSCH, F. HULLIGER and U. WINKLER, *Helv. Phys. Acta* **27** (1954) 249.
27. O. RECHEWEG, C. LIND, A. SIMON and F. J. DISALVO, *Zeit fur Naturforschung B –J. Chem.. Sci*. **58** (2003) 159.
28. P. LARSON and S. D. MOBANTI, *Phys. Rev*. **B59** (1999) 15660.
29. Y. IMAI, M. MUKAIDA and T. TSUNODA, *Intermetallics* **8** (2000) 381.
30. F. AYMERICH and G. MULA, *Phys. Stat. Sol*. **42** (1970) 697.
31. G. M. FEHRENBACK and H. BROSS, *Eur. Phys. J*. **B 9** (1999) 37.
32. A. MOKHTARI and H. AKBARZADEH, *Physica B* **337** (2003) 122.
33. A. M. HEYNS, L. C. PRINSLOO, K.–J. RANGE and M. STASSEN, *J. Solid State Chem*. **137** (1998) 33.
34. D. J. MIN and N. SANO, *Met. Trans*. **B19** (1988) 433.

Received 5 August 2004
and accepted 13 July 2005